Novel cost-efficient protein-membrane based system for cells co-cultivation and modeling the intercellular communication

A Minin[1,2*] | I Blatov[3] | V Lebedeva[3] | M Tuchai[4] |
V Pozdina[5] | I Zubarev[3,6*]

[1]M. N. Mikheev Institute of Metal Physics, Yekaterinburg, Russian Federation

[2]Ural Federal University, Yekaterinburg, Russian Federation

[3]Moscow Institute of Physics and Technology, Dolgoprudny, Russian Federation

[4]Ural Research Center for Radiation Medicine, Chelyabinsk, Russian Federation

[5]Institute of Immunology and Physiology, Yekaterinburg, Russian Federation

[6]Lomonosov Moscow State University, Moscow, Russian Federation

Correspondence
I Zubarev PhD, Moscow Institute of Physics and Technology, Dolgoprudny, Russian Federation
Email: ilyamitozubarev@gmail.com

Funding information
Russian Science Foundation Grant #19-74-00081

In vitro systems serve as compact and manipulate models to investigate interactions between different cell types. A homogeneous population of cells predictably and uniformly responds to external factors. In a heterogeneous cell population, the effect of external growth factors is perceived in the context of intercellular interactions. Indirect cell co-cultivation allows one to observe the paracrine effects of cells and separately analyze cell populations. The article describes an application of custom-made cell co-cultivation systems based on protein membranes separated from the bottom of the vessel by the 3d printed holder or kept afloat by a magnetic field. Using the proposed co-cultivation system, we analyzed the interaction of A549 cells and fibroblasts, in the presence and absence of growth factors. During co-cultivation of cells, the expression of genes of the activation for epithelial and mesenchymal transitions decreases. The article proposes the application of a newly available system for the co-cultivation of different cell types.

KEYWORDS
cell matrix, magnetic nanoparticles, EMT, RT-PCR, 3d printing

1 | INTRODUCTION

Cell-to-cell interactions within different cell types could be studied in vitro. Controlled conditions provide a simplified system that can model basic cellular responses to reciprocal paracrine signals. In the cells co-cultivation system, it is possible to model the processes of an epithelial-mesenchymal transition (EMT), in which a polarized epithelial cell undergoes a series of changes, resulting in a high mobility mesenchymal cell. At the initial stage of transition, the cells acquire an intermediate epithelial/mesenchymal phenotype with both epithelial and mesenchymal properties. During EMT, gene expression changes and there is a loss of adhesive cell-cell contacts, leading to increased migration and invasion. Modeling the EMT process makes it possible to understand the mechanisms underlying it, which could be useful for early diagnosis of cancer and clinical control. In vitro, controlled EMT induction is a useful tool for drug screening, identifying genes involved in the transition process, and studying the resistance of cancer cells to therapeutic drugs [1].

Paracrine interactions between the cancer epithelial cell and normal fibroblasts lead to a mutual change in the phenotype of both cell populations. Additionally, paracrine interactions can alter the sensitivity and response of cells to changes in cell culture conditions. Fibroblasts, exposed to paracrine signals from the changing epithelial cells, activate and start to dynamically interact with cancer cells, promoting tumor progression [2]. These cancer-associated fibroblasts (CAFs) produce an excessive amount of extracellular matrix, forming a very dense stroma, and acquire an activated phenotype through the expression of activation markers such as α-smooth muscle actin (α-SMA), fibroblast activation protein (FAP), and fibroblast-specific protein 1 (FSP1), S100A4, PDGFRα / β, tenascin-C, neuron glial antigen (NG2), desmin, CD90 / THY1, and podoplanin (PDPN) [3, 4]. Besides, CAFs act epigenetically on cancer cells through the epithelial-mesenchymal transition [5]. The different ability to induce EMT has shown for populations of fibroblasts [6] : breast cancer tissue fibroblasts differ from normal fibroblasts in their ability to effectively induce a high level of EMT [7]. Thus, various factors released by fibroblasts can support the proliferation and invasion of tumor cells [8].

Autocrine factors produced by fibroblasts maintain epithelial phenotype, survival, and proliferation of tumor cells. During bidirected paracrine interaction between cells, their response to growth factors (GF) can change significantly. Several growth factor receptors (epidermal growth factor (EGF), platelet-derived growth factor (PDGF), fibroblast growth factor (FGF), transforming growth factor β-1 (TGFβ-1)) are over-expressed during the progression of cancer [9]. Many growth factors have been shown to be involved in the induction and progression of cancer. This influence is determined by the cellular environment, which can regulate the stimulated action of growth factors. Induction of initial stages and progression of EMT in vitro can be achieved by adding different growth factors (EGF, FGF-10, PDGF-D, TGFβ-1).

EGF decreases the expression of the E-cadherin protein in epithelial cells as well as activates Zeb1 / ERK / MAPK [10]. EGF increases proliferation, mediates invasion of epithelial cells [11], fibroblasts migration and contractility in vitro [12]. FGF-10 is a well-known protein involved in the organogenesis of many organs, such as the lungs and the progression of EMT. In cell lines, FGF-10 regulates and induces EMT through various types of signaling pathways [13, 14]. FGF10/FGFR2 induces cell migration and invasion in cancer epithelial cells [15] and regulates mesenchymal cell differentiation (16). PDGF-D plays a key role in the development and progression of human malignant tumors. PDGF-D can stimulate EMT in cell culture and during malignant transformation in vivo, which is accompanied by a decrease in E-cadherin and increased vimentin expression [16]. PDGF-D overexpression led to increased epithelial cell invasion, cell proliferation, migration, angiogenesis, and metastasis [17] as well as recruitment, proliferation, and functional activities of fibroblasts [18]. TGFβ-1 treatment significantly increases cell proliferation, promotes various cancer cell invasive and cancer stem cell phenotypes [19, 20, 21]. TGF-β1 promotes the proliferation, collagen formation, tumor

growth, and metabolic reprogramming of tumor microenvironment - cancer-associated fibroblasts [20, 22].

In this study, we show the influence of the above growth factors on fibroblast and epithelial cell cultures with and without a co-cultivation. In our previous study [23], we discuss the development of a prototype of a cell co-cultivation system based on a protein membrane. There are several commercially available co-cultivation systems for studying the paracrine effects between different cell lines, but they are expensive and not available to all laboratories. Using three-dimensional (3D) printing, it is possible to create an analog of such a system. 3D printing technology is widely used to solve scientific problems and allows quickly and affordably to produce specially designed models for in vitro experiments. The article shows the application 3D printing-derived protein membranes as systems for co-cultivation of cells.

2 | MATERIALS AND METHODS

2.1 | Synthesis and modification of nanoparticles

Metal-carbon nanoparticles (MNPs) Fe@C were synthesized by using the gas-condensation technique as described [24], in the applied magnetism laboratory of the Institute of Metal Physics, Ural Division of the Russian Academy of Sciences. The size of the iron-carbon nanoparticles is about 10 nm in diameter [24]. The diameter of the core, which consists predominantly of alpha iron, is about 8 nm. The saturation magnetization of these nanoparticles is about 100 emu/g, which is higher than that of iron nanoparticles often used in biology (about 70-80 emu/g), which makes it possible to impart a greater magnetic moment to the membrane without overloading it with particles. To bind to the protein, metal-carbon nanoparticles were modified with amino groups, according to the technique described in detail elsewhere [25]. Briefly, derivatives of aryldiazonium, in this case, para-aminobenzoic acid, are used to modify nanoparticles. Sodium nitrite under acidic conditions converts the amino group of PABA into a diazo group, which is conjugated with the carbon shell of the nanoparticles, while the carboxyl group of the molecule sticks out. The carboxyl group allows the particles to be hydrophilized, which stabilizes their aqueous suspension, and allows subsequent conjugation with proteins.

2.2 | 3d printing of primary mold

MSLA (masked stereolithography) 3D printers Photon (Anycubic, China), and Mars (Elegoo, China) were used to form the primary molds with controlled shape and size. The printer firmware has been updated to the latest version. Primary molds were printed on MSLA 3d printers (Photon, Anycubic, China) from standard gray SLA resin (Anycubic, China) than cured with UV light. The models were printed with a vertical resolution of 25 microns, in a flat orientation, as this provides the maximum smoothness of the mold surface.

For the preparation of secondary molds, two-component minimally viscous Alcorsil 315 silicone (Alcorsil, China) was added to the primary ones. We used 2% of the hardener, as this provides maximum ease of use with adequate density of the final mold. After hardening, the secondary silicone molds were washed in 99% isopropanol to remove any impurities. Images of the model of the primary mold and its photographs are shown in the supplementary materials (S3, S4, S5).

To prevent cell migration, a wall with a height of about $200 \mu m$ was made at the edge of the membrane (Figure 1). This was done by modifying the primary mold 3d model accordingly. This was done by adding to the 3D model a primary mold of a wall with a height of 200 microns along the periphery.
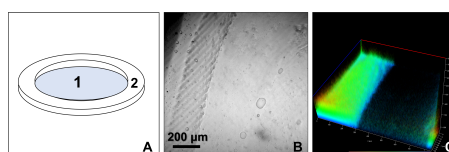
FIGURE 1 A - a sketch of the membrane (1 - useful membrane space, 2 - a wall that prevents cells from migrating from the membrane). B - image of the wall at the edge of the membrane obtained with an optical microscope and 3d reconstructed image obtained using z-stack confocal microscopy(C).
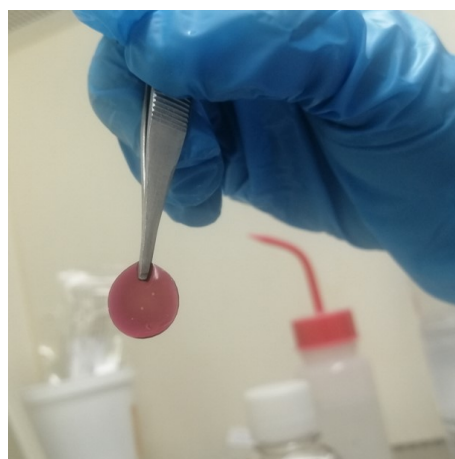

FIGURE 2 Freshly produced membrane after washing with DMEM.

2.3 | Protein membranes preparation

BSA 20% solutions, aminated nanoparticles, and EDC (1-(3-Dimethylaminopropyl)-3-ethylcarbodiimide hydrochloride) crosslinker were placed in silicone forms. 25/mul of iron-carbon nanoparticles, grafted with carboxy groups (4 mg/ml) is added to 1 ml of the solution BSA and sterilized through a 0.22/mum filter. Membrane polymerization was carried out in silicone molds.

The components were premixed in 1 ml microcentrifuge tubes. There were placed 100 mg of EDC and 600/mul of the suspension of the protein with nanoparticles. The mixture was quickly mixed with a vortex until homogeneous and centrifuged to remove bubbles (3000 RCF, 4 degrees Celsius). Then the suspension was transferred using a dispenser into three silicone molds, 200/mul each, and carefully distributed over them. Polymerization lasted for 24 hours at room temperature in a humid atmosphere. To maintain humidity, the molds were placed in a plastic container with a small amount of water. A humid atmosphere is necessary to prevent uneven drying of the membrane, which leads to its twisting and unsuitability for further use.

The fully polymerized membrane was carefully separated from the silicone mold by stretching and bending the mold itself by hand. Attempts to separate the membrane with tweezers often led to its rupture. Polymerized protein membranes were rinsed by sterile deionized water and soaked two days in a complete tissue culture medium.

Photos of polymerized and rinsed with DMEM membranes are shown in Figure 2, and stages of the membrane's production shown in support materials (S6), include a failed crooked membrane after air dried (S7).

subsectionMagnetic membrane support A magnetic non-volatile system for magnetically controlled cell co-cultivation was constructed based on commercially available permanent NdFeB magnets. The system was constructed with three magnets: two a cylindrical permanent magnet (d = 50 mm, h = 20 mm) to improve the uniformity of the magnetic field and increase the field above the magnet, and a cylindrical permanent magnet (d = 10 mm, h = 3 mm). The total magnetic field can obtain the optimal configuration of the magnetic field, with the highest magnetic field strength in the projection of the center of the system for holding a magnetically controlled membrane at the phase boundary (Image 3A and, in the center of the dish. The magnetic system is placed inside the box printed on a 3D printer made of PLA plastic, equipped with interchangeable supports of different heights. The photograph 3A of the magnetic system are given in the supplementary materials (S8). The work used a magnetic system for petri dishes, however, a magnetic system was also developed capable of supporting multiple membranes in a 24 well plate (S1, S2).

The plastic membrane holders were printed on an FDM printer (CR-10s, CR-6SE, Creality, China) in a PLA plastic (Bestfilament, Russia). Details of the holder's construction are given in the supporting materials (S8(. Photos of the plastic insert are shown in the figure 3B.

2.4 | Membranes permeability and capacity study

To study the capacity and permeability of membranes for low-molecular molecules, methylene blue dye (Sigma-Aldrich, USA) was used [26].

First, the membrane was saturated in methylene blue solution (500 mM) for a day, after which the excess dye was removed using filter paper, and the membrane was placed in a Petri dish with phosphate-buffered saline (pH = 7.4). To study the permeability the membrane was placed in a holder (printed on an FDM 3d printer) fixed on a plastic dish 4 , and immersed in a culture medium. Above the membrane in a holder was placed 500 μL of methylene blue solution with a concentration of 50 mM. Solution samples were taken at regular intervals and the concentration of the dye was determined by spectrophotometry (SF-102, NPK Akvilon, Russia).

The dye capacity of the membrane was determined by the amount of substance that the membrane released into the solution. Experiments on the release of the dye from the saturated membrane and on the passage of the dye through the membrane were carried out in an incubator at a temperature of 37 degrees, in five iterations.

2.5 | Cell cultures

A549, HeLa, HEK 293, MiaPaca 2 cell line and Human foreskin fibroblasts (HFF) were obtained from the Russian cell cultures collection of the Institute of Cytology RAS (Russia, St. Petersburg). The cells were maintained in plastic vials containing culture medium (DMEM) with 10% FBS and $50/mu$g / ml gentamicin, in an incubator at + 37 ∘ C, 5% CO2. Co-culturing of A549 and HFF cells was performed in a Petri dish with a magnetic system on top. The magnetic holder enables maintenance of levitation of the protein membrane with nanoparticles in the volume of the culture medium, closer to the liquid-air interface. Growth effects of peptides were determined by incubating cells for 4 days with peptides in the serum-free medium after a 72-h preincubation in 10% serum-supplemented medium alone. Recombinant human growth factors were used at concentrations with biological activity: PDGF 50 ng/ml, TGFb 2 ng/ml, EGF 25 ng/ ml, FGF10 50 ng/ml. During co-cultivation, A549 grew on the membrane, while fibroblasts on the bottom of a multi-well plate.
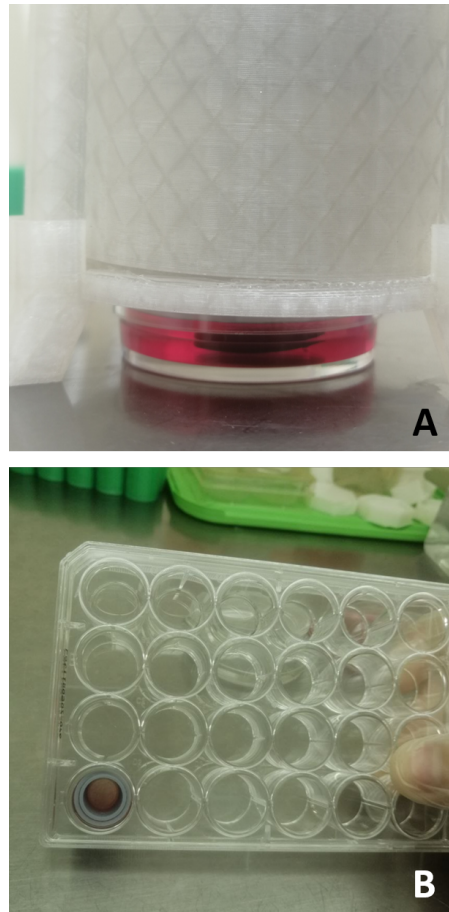
FIGURE 3 Magnetic membrane floating under a magnetic system in a dish (A) and a membrane in a SLA 3d-printed cylindrical insert inside a 24 well plate (B).

2.6 | Cell viability assessment

MTT assay was carried out for assessing cell metabolic activity. Membranes with a monolayer of cells were washed thrice with cultured medium, moved into a clean 24-well plate, and then, 1 ml of medium and 0.5 mg/ml MTT (Biolot, Russia) were added into each well (37∘C for 4 h). After incubation, in each well, the medium was removed and replaced with 1 ml DMSO (Panreac, Spain) and left for 15 min long incubation. The plate was read within 1 h at OD = 590 nm using a Lazurit plate reader spectrophotometer (Vector-Best, Russia). Membranes without cells, whether loaded with particles or not, did not give a significant color change under similar conditions.

2.7 | RNA isolation, reverse transcription and RT-qPCR.

A Trypsin-EDTA solution (Gibco, USA) was used to separate the cells from the membrane. Then the solution with the cells was centrifuged to precipitate them.
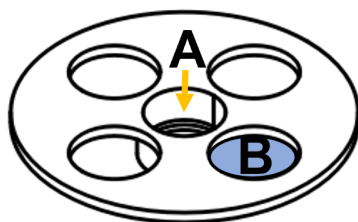
FIGURE 4 Sketch of special holder for studying membrane permeability. A - hole with membrane, B - hole for sampling.

For purification of high-quality RNA from cells we used silica-membrane RNeasy spin columns (RNeasy Mini Kit, QIAGEN, Germany) with DNAase in column digestion according to manufacturer's instructions. RNA integrity was controlled by agarose gel electrophoresis. For reverse transcription 2 μg of the isolated RNA was used. Reverse transcription was carried out with the iScript gDNA Clear cDNA Synthesis Kit (Bio-Rad Laboratories, Inc., United States) according to the manufacturer's instructions. For qPCR 1 μl of the cDNA of each sample was pipetted into a 96-well qPCR plate, 1 μl each primer primer (Lumiprobe RUS, Russia) (list of primers given in Table S9) , and 22 μl of a master mix solution. GAPDH was used as a housekeeping gene, water, and RNA as negative controls were included. Change in gene expression was determined by using the Δ Δ Ct method.

3 | RESULTS AND DISCUSSION

3.1 | Permeability and capacity of membranes

For a dye free floating membrane, the process of release of a substance has a two-stage regularity. At first, methylene blue is released quickly, about a third of the total amount goes into solution in the first hour. This is explained by dye accumulated in the pores of the membrane. The further release is slower and the concentration of the dye in the membrane and the solution is completely equalized within two days. From these data, the membrane capacity for methylene blue was also determined about 200 ng/mm^3. The change in the concentration of dye in solution for different experiments is shown in the figure below.

Also permeability of the membrane in plastic holder for the methylene blue was studied. In the beginning, the process occurs rather slowly, since the dye saturates the membrane, and only after that it relatively slow goes into the buffer.

Nevertheless, within about a day, the concentration of methylene blue is equal in the compartments separated by the membrane. Thus, it was shown that the protein membrane is permeable to low-molecular substances, which is important for its use in co-cultivation of cells. It should be noted that low molecular weight molecules can accumulate in the membrane and then will be slowly realized.

3.2 | Cells on membranes

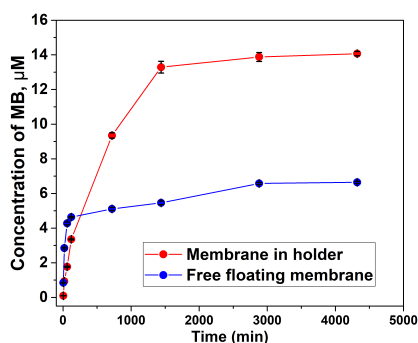The general design of the biologincal experiments performed is shown in the figure 7.

FIGURE 5 Release of the dye from the pre-saturated membraneand the passage of the dye through the membrane in the holder

BSA protein has been used as a main component to create the membranes. The BSA with magnetic nanoparticles was polymerized in silicone form and thin and protein membranes were obtained (Fig. 2). To avoid membrane deformation, it is important to ensure uniform protein polymerization. When it dries quickly, the membrane polymerizes unevenly and deforms during washing (S7). Polymerization in a humid atmosphere or inside silicone forms smooth membranes. These membranes are optically transparent, cells are clearly visible on the surface in the light microscope (Fig. 8). The biocompatibility of the 3D printing materials on the cells has been tested in a previous article ([27]). The price of one membrane is less than 1 USD, which is almost an order of magnitude cheaper than the Transwell systems (Corning, USA).

Cells were seeded and adhered to the surface of the membrane in a 24-well plate. After four days of cultivation, a monolayer of cells was formed on the membrane, and the edge migration of cells stopped. A magnetic holder was used to levitate protein membranes with cells in the volume of the cultured medium. Used magnets are very strong, and must be handled with extreme care so that they are not magnetized anywhere. In addition to the magnetic holder for one Petri dish, a model of the magnetic holder for a multi-well plate was proposed. A diagram of the device of this system, as well as numerical modeling of the magnetic field optimal for maintaining magnetically controlled membranes in it, are given in the supplementary materials (S1, S2). In this work, we do not consider the effect of a magnetic field on cells, since, according to literature data, the effect of a constant magnetic field of such strength does not affect biological processes in cells [28, 29].

To prevent cell migration, a wall with a height of 200 μm was made at the edge of the membrane. During short-term cell cultivation on a levitating membrane in DMEM-F12 (4 days) no migration of cells from the membrane to the bottom of the culture vessel was detected.

Comparison of the viability of different cell lines during growth on magnetically controlled membranes and standard culture plates. This effect is due to the slightly smaller available area for cell growth. The results of the MTT test are shown in Figure 9.

Alternatively, 3D printed plastic cylindrical inserts have been constructed. The protein membrane can be inserted between two cylinders and cling to the edge of the culture well (Fig. 3B). All technological data for the manufacture of magnetic systems and cylindrical inserts are presented in the materials (S3). Both proposed systems for co-cultivation of cells have some advantages and limitations. Their comparison is shown in Table 1.

According to the membrane permeability, we have chosen only one cell co-cultivation system with magnetic nanoparticles. In such a membrane, the diffusion of molecules occurs in all directions and faster, that is important for
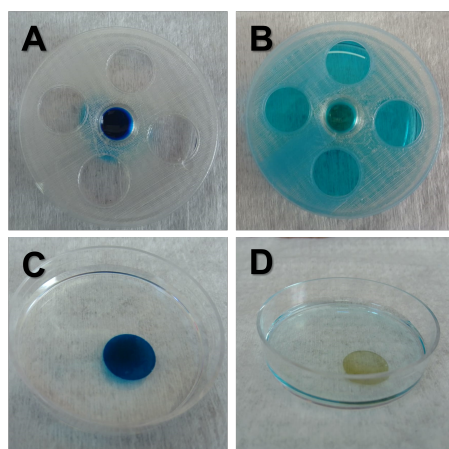
FIGURE 6 Photographs of membranes in the holder for permeability studies (A and B). A - 30 minutes after adding the dye, B - after 72 hours. C and D - dye-saturated membranes, C - 5 minutes after incubation in PBS, D - 72 hours

short-lived molecules.

3.3 | Cell co-cultivation

Epithelial cells (A549) and human foreskin fibroblasts (HFF) were used in the experiment. Fibroblast cells and A549 co-cultivated on membranes in a magnetic field. We assessed the effect of growth factors (EGF, FGF-10, PDGF-D, TGFβ-1) on individual cell populations and during co-cultivation of cells (Fig. 10). Individual cell lines were used as controls and were grown without additional growth factors. 22 samples were isolated: cultures of A549 and HFF cells (intact cells, 4 GF for each cell line - 10 samples), co-cultivation of A549 and HFF cells (intact cells, 4 GF and a GF combination - 12 samples). Using our co-culture systems, we evaluate the influence of these factors on individual cell lines and their co-culture.

In epithelial cells, the expression of vimentin, fibronectin, Snail, Zeb1, and E-cadherin was used to analyze the epithelial-mesenchymal transition by quantitative PCR (qPCR). The household reference gene was taken by GAPDH. Several key activation proteins were assessed in fibroblasts: α-smooth muscle actin (α-SMA), fibroblast activation protein (FAP), and fibroblast specific protein 1 (FSP1). qPCR has shown that a change in normal human fibroblasts affects epithelial cells with paracrine factors (Fig. 10).

Among all growth factors, the addition of FGF-10 to A549 cells caused the most dramatic changes, resulting in the increased gene expression profile of vimentin, fibronectin, Snail1, and Zeb1. A less pronounced effect was for TGFβ-1 and EGF, which is typical for EMT. However, there is a multifaceted effect of FGF-10 and other growth factors on the expression of E-cadherin: FGF-10 activates it, while other factors suppress it. The involvement of FGF-10 in the morphogenesis of the lung tissue from which this cell line originates can be a potential explanation of this interaction [30]. During co-cultivation, epithelial cells change the response of A549 cells to growth factors. In most samples, the expression of fibronectin and vimentin decreases and is enhanced only by the addition of TGFβ-1. This is especially noticeable when cells are co-cultured in the absence of additional growth factors. The addition of exogenous factors supports cell activation and EMT: EMT markers (Snail1 and Zeb1) are increased by all growth
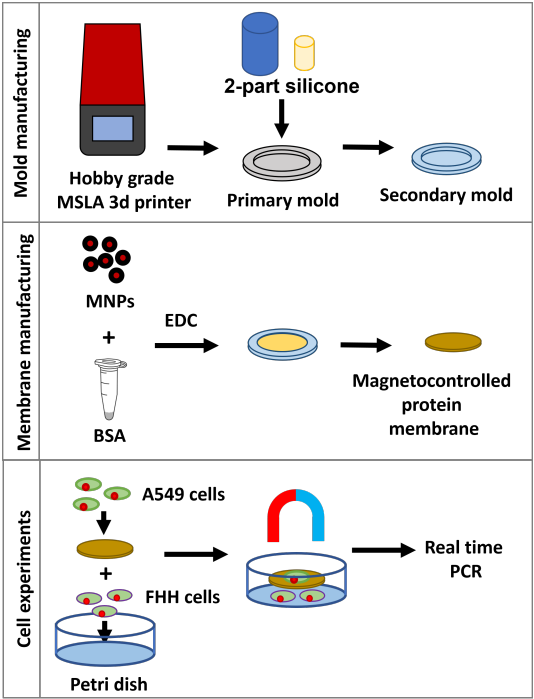
FIGURE 7 Experiment design diagram

factors during cell co-culture. The strongest influence on the induction of Snail1 and Zeb1 was the addition of TGFβ-1 to the culture medium. At the same time, the expression of E-cadherin decreased in all samples under the influence of growth factors and upon co-cultivation of cells. Intercellular interactions of different cell types resulted in a loss of sensitivity to FGF-10 and an increase in the response to TGFβ-1. Thus, in all samples during cell co-cultivation, the initiation and progression in EMT genes expression are noted. Interestingly, co-cultivation of cells without growth factors inhibits the processes of EMT and cell activation, and the transcription level of markers decreases. The cells are likely to secrete soluble growth factors that determine the mutual inhibition of EMT.

The addition of any growth factors to fibroblasts caused activation of expression aSMA, FAP, and FSP1. TGFβ-1 has the strongest effect on enhancing the expression of aSMA and slightly suppresses the expression of FSP1, which is consistent with its fibrogenic properties [31]. FGF10 expression is reduced in many samples; however, the addition of FGF10 itself to the culture medium enhances its expression, which indicates the presence of a positive feedback loop in fibroblasts [32]. During co-cultivation of epithelial cells and fibroblasts, paradoxical changes in the gene expression profile are observed. The expression of aSMA is markedly reduced, the expression of FGF10 disappears. With the addition of TGFβ-1, the level of FAP expression is maintained relative to a culture of fibroblasts, while FSP1 is decreased. When cells are co-cultured without growth factors and in the presence of EGF, FGF-10, PDGF-D, the opposite picture is observed: the level of FAP expression decreases, but FSP1 is retained.

Thus, the effect of growth factors on individual cell populations and co-cultivation showed different biological activities. It is clearly shown that the presence of different types of cells and intercellular communication completely changes the response to growth factors. One of the possible mechanisms of changes in the sensitivity of cells during
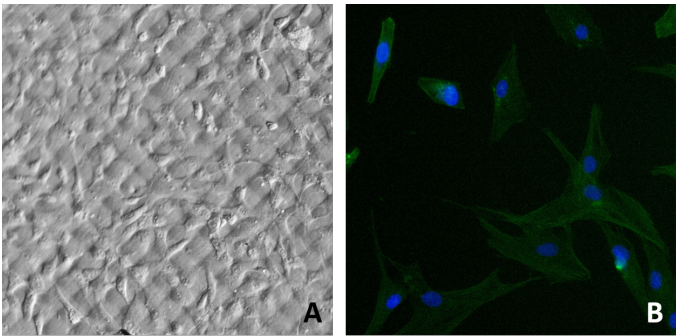
FIGURE 8 A549 cell culture on the membrane. A - bright field. Square pixels are clearly visible as a result of the primary form printing on the MSLA printer. B - fluorescent image of the cells. Blue - nucleus, green - cytoskeleton (actin)
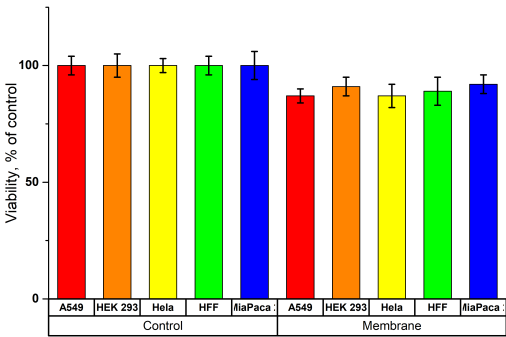

FIGURE 9 Comparison of cell viability of different cell lines grown on magnetically controlled membranes and on standard culture plates

co-cultivation to growth factors is the competition of receptors for added molecules of growth factors. The changes obtained in the experiment show the importance of the context of intercellular interactions. Short-term co-cultivation of normal fibroblasts and tumor cells resulted in suppression of the activity of both types of cells. It may take more time to change the physiology of fibroblasts to a CAF-positive phenotype. The application of systems for co-cultivation of different cell types makes it possible to analyze the common influence on the physiology of cells. Our multicellular co-culture system can be fabricated in any laboratory using 3D printing and available reagents. It can be used to simulate paracrine interactions between different cell types.

4 | CONCLUSION

A technique was developed for creating biocompatible protein membranes that can be used for co-cultivation of cells. The article studies the capacity and permeability of these membranes for low molecular weight substances and shows

TABLE 1 Comparison of co-cultivation systems: magnetic and based on cylindrical inserts

| Characteristic	Magnetic co-culture system (5'→ 3')	Inserts system
Sterilization	No additional parts in the culture medium (no need to sterilization)	Plastic parts (cylinders) must be sterilized. The plastic used is not autoclavable and degrades with aggressive disinfectants. It can be treated with UV or gamma rays.
Useful area	The area is limited by the diameter of the well	The usable area is less. Limited by the size of the insert.
Convenience for manipulation	It is necessary to remove the membrane by tweezers.	Removable plastic insert allows easy removal of the membrane
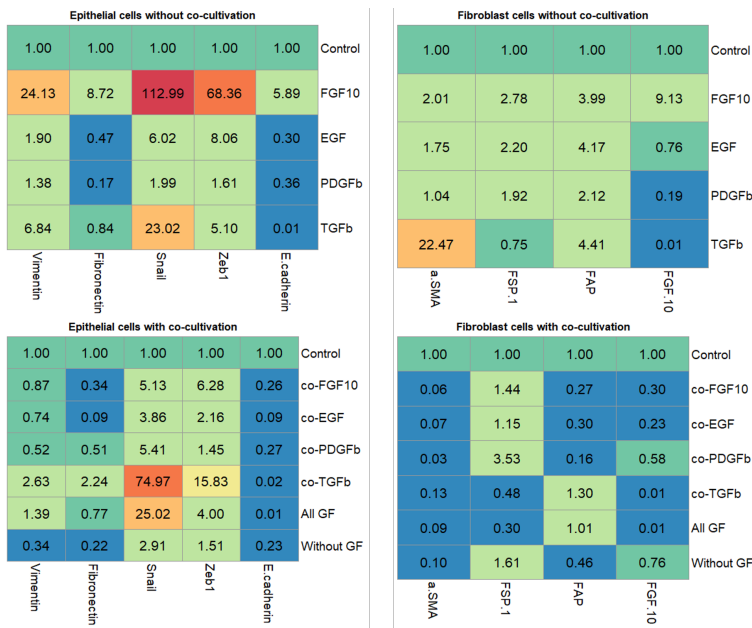
FIGURE 10 PCR data heat map. Data shown for individual cell lines and combined cultivation. Control (separate cell line without grown factors), cell with grown factors (EGF, FGF-10, PDGF-D, TGFβ-1), cell co-cultivation with grown factors (co-EGF, co-FGF-10, co-PDGF-D, co-TGFβ-1, all grown factors) and cell co-cultivation without grown factors (explanations in the text)

their ability to accumulate and gradually release low molecular weight substances. For the model substance used in this experiment (methylene blue), the capacity was approximately 200 ng/mm^3.

In our model system for co-cultivation using epithelial and fibroblast cells, we have shown that the action of

growth factors changes during cell-to-cell interaction. Intercellular paracrine interactions may be critical in regulating the response to soluble growth factors. The proposed models for cell co-cultivation make it possible to study the paracrine effect on the morphological and biochemical states of separated cell populations. The cell co-cultivation systems described in this article can be produced in any laboratory and provides an economical alternative to commercially available membrane inserts.

Acknowledgements

Conflict of interest

There are no conflicts to declare.

references

[1] Kalluri R, Weinberg RA, et al. The basics of epithelial-mesenchymal transition. The Journal of clinical investigation 2009;119(6):1420–1428.

[2] Eiro N, González L, Martínez-Ordoñez A, Fernandez-Garcia B, González LO, Cid S, et al. Cancer-associated fibroblasts affect breast cancer cell gene expression, invasion and angiogenesis. Cellular Oncology 2018;41(4):369–378.

[3] Von Ahrens D, Bhagat TD, Nagrath D, Maitra A, Verma A. The role of stromal cancer-associated fibroblasts in pancreatic cancer. Journal of hematology & oncology 2017;10(1):1–8.

[4] Chen X, Song E. Turning foes to friends: targeting cancer-associated fibroblasts. Nature reviews Drug discovery 2019;18(2):99–115.

[5] Nair N, Calle AS, Zahra MH, Prieto-Vila M, Oo AKK, Hurley L, et al. A cancer stem cell model as the point of origin of cancer-associated fibroblasts in tumor microenvironment. Scientific reports 2017;7(1):1–13.

[6] Gao MQ, Kim BG, Kang S, Choi YP, Park H, Kang KS, et al. Stromal fibroblasts from the interface zone of human breast carcinomas induce an epithelial–mesenchymal transition-like state in breast cancer cells in vitro. Journal of cell science 2010;123(20):3507–3514.

[7] Soon P, Kim E, Pon CK, Gill AJ, Moore K, Spillane AJ, et al. Breast cancer-associated fibroblasts induce epithelial-to-mesenchymal transition in breast cancer cells. Endocr Relat Cancer 2013;20(1):1–12.

[8] Metzler VM, Pritz C, Riml A, Romani A, Tuertscher R, Steinbichler T, et al. Separation of cell survival, growth, migration, and mesenchymal transdifferentiation effects of fibroblast secretome on tumor cells of head and neck squamous cell carcinoma. Tumor Biology 2017;39(11):1010428317705507.

[9] Wong HH, Lemoine NR. Pancreatic cancer: molecular pathogenesis and new therapeutic targets. Nature reviews Gastroenterology & hepatology 2009;6(7):412.

[10] Devaraj V, Bose B. Morphological state transition dynamics in EGF-induced epithelial to mesenchymal transition. Journal of clinical medicine 2019;8(7):911.

[11] Shirk AJ, Kuver R. Epidermal growth factor mediates detachment from and invasion through collagen I and Matrigel in Capan-1 pancreatic cancer cells. BMC gastroenterology 2005;5(1):1–13.

[12] Kim D, Kim SY, Mun SK, Rhee S, Kim BJ. Epidermal growth factor improves the migration and contractility of aged fibroblasts cultured on 3D collagen matrices. International journal of molecular medicine 2015;35(4):1017–1025.

[13] Abolhassani A, Riazi GH, Azizi E, Amanpour S, Muhammadnejad S, Haddadi M, et al. FGF10: type III epithelial mesenchymal transition and invasion in breast cancer cell lines. Journal of Cancer 2014;5(7):537.

[14] Qazvini FF, Samadi N, Saffari M, Emami-Razavi AN, Shirkoohi R. Fibroblast growth factor-10 and epithelial-mesenchymal transition in colorectal cancer. EXCLI journal 2019;18:530.

[15] Nomura S, Yoshitomi H, Takano S, Shida T, Kobayashi S, Ohtsuka M, et al. FGF10/FGFR2 signal induces cell migration and invasion in pancreatic cancer. British journal of cancer 2008;99(2):305–313.

[16] Wu J, Chu X, Chen C, Bellusci S. Role of fibroblast growth factor 10 in mesenchymal cell differentiation during lung development and disease. Frontiers in genetics 2018;9:545.

[17] Wang Z, Banerjee S, Li Y, Rahman KW, Zhang Y, Sarkar FH. Down-regulation of Notch-1 inhibits invasion by inactivation of nuclear factor-κB, vascular endothelial growth factor, and matrix metalloproteinase-9 in pancreatic cancer cells. Cancer research 2006;66(5):2778–2784.

[18] Rajkumar VS, Shiwen X, Bostrom M, Leoni P, Muddle J, Ivarsson M, et al. Platelet-derived growth factor-β receptor activation is essential for fibroblast and pericyte recruitment during cutaneous wound healing. The American journal of pathology 2006;169(6):2254–2265.

[19] Kali A, Ostapchuk YO, Belyaev NN. TNFα and TGFβ-1 synergistically increase the cancer stem cell properties of MiaPaCa-2 cells. Oncology letters 2017;14(4):4647–4658.

[20] Liu Y, Li Y, Li N, Teng W, Wang M, Zhang Y, et al. TGF-β1 promotes scar fibroblasts proliferation and transdifferentiation via up-regulating MicroRNA-21. Scientific reports 2016;6(1):1–9.

[21] Tirino V, Camerlingo R, Bifulco K, Irollo E, Montella R, Paino F, et al. TGF-β 1 exposure induces epithelial to mesenchymal transition both in CSCs and non-CSCs of the A549 cell line, leading to an increase of migration ability in the CD133+ A549 cell fraction. Cell death & disease 2013;4(5):e620–e620.

[22] Guido C, Whitaker-Menezes D, Capparelli C, Balliet R, Lin Z, Pestell RG, et al. Metabolic reprogramming of cancer-associated fibroblasts by TGF-β drives tumor growth: connecting TGF-β signaling with "Warburg-like" cancer metabolism and L-lactate production. Cell cycle 2012;11(16):3019–3035.

[23] Minin A, Blatov I, Rodionov S, Zubarev I. Development of a cell co-cultivation system based on protein magnetic membranes, using a MSLA 3D printer. Bioprinting 2021;23:e00150. `https://www.sciencedirect.com/science/article/pii/S2405886621000233`.

[24] Yermakov AY, Uimin MA, Byzov IV, Konev AS, Novikov SI, Minin AS, et al. Structure and magnetic properties of carbon encapsulated FeCo@C and FeNi@C nanoparticles. Materials Letters 2019;254:202–205.

[25] Postnikov PS, Trusova ME, Fedushchak T, Uimin M, Ermakov A, Filimonov VD. Aryldiazonium tosylates as new efficient agents for covalent grafting of aromatic groups on carbon coatings of metal nanoparticles. Nanotechnologies in Russia 2010;5(7):446.

[26] Chung A, Rubner M. Methods of loading and releasing low molecular weight cationic molecules in weak polyelectrolyte multilayer films. Langmuir 2002;18(4):1176–1183.

[27] Minin A, Blatov S, Rodionov S, Zubarev I. Development of a cell co-cultivation system based on protein magnetic membranes, using a MSLA 3D printer. Bioprinting 2021;p. e00150.

[28] Blyakhman FA, Melnikov GY, Makarova EB, Fadeyev FA, Sedneva-Lugovets DV, Shabadrov PA, et al. Effects of constant magnetic field to the proliferation rate of human fibroblasts grown onto different substrates: Tissue culture polystyrene, polyacrylamide hydrogel and ferrogels γ-Fe2O3 magnetic nanoparticles. Nanomaterials 2020;10(9):1697.

[29] Fei Y, Su L, Lou H, Zhao C, Wang Y, Chen G. The effects of 50 Hz magnetic field–exposed cell culture medium on cellular functions in FL cells. Journal of radiation research 2019;60(4):424–431.

[30] Yuan T, Volckaert T, Chanda D, Thannickal VJ, De Langhe SP. Fgf10 signaling in lung development, homeostasis, disease, and repair after injury. Frontiers in genetics 2018;9:418.

[31] Border WA, Noble NA. Transforming growth factor β in tissue fibrosis. New England Journal of Medicine 1994;331(19):1286–1292.

[32] Jin L, Wu J, Bellusci S, Zhang JS. Fibroblast growth factor 10 and vertebrate limb development. Frontiers in genetics 2019;9:705.